PHYSICAL REVIEW B **93**, 241410(R) (2016)

# Ferromagnetism and superconductivity with possible $p + ip$ pairing symmetry in partially hydrogenated graphene

Hong-Yan Lu,[1,2,*] Lei Hao,[1,3] Rui Wang,[1,4] and C. S. Ting[1]

[1]*Texas Center for Superconductivity and Department of Physics, University of Houston, Houston, Texas 77204, USA*

[2]*School of Physics and Electronic Information, Huaibei Normal University, Huaibei 235000, China*

[3]*Department of Physics, Southeast University, Nanjing 210096, China*

[4]*National Laboratory of Solid State Microstructures and Department of Physics, Nanjing University, Nanjing 210093, China*

(Received 12 February 2016; revised manuscript received 11 June 2016; published 29 June 2016)

By means of first-principles calculations, we predict two new types of partially hydrogenated graphene systems: $C_6H_1$ and $C_6H_5$, which are shown to be a ferromagnetic (FM) semimetal and a FM narrow-gap semiconductor, respectively. When properly doped, the Fermi surface of the two systems consists of an electron pocket or six hole patches in the first Brillouin zone with completely spin-polarized charge carriers. If superconductivity exists in these systems, the stable pairing symmetries are shown to be $p + ip$ for both electron- and hole-doped cases. The predicted systems may provide fascinating platforms for studying the novel properties of the coexistence of ferromagnetism and triplet-pairing superconductivity.

DOI: 10.1103/PhysRevB.93.241410

*Introduction.* In recent years, hydrogenation of graphene has attracted increasing interest because it can modify the electronic and magnetic properties of graphene, providing a possible way for functioning graphene to have specially designed features. For example, fully hydrogenated graphene (graphane), with hydrogen atoms bonded to carbon atoms alternatively on both sides of the carbon plane, was theoretically predicted [1] and experimentally synthesized by exposing graphene in hydrogen plasma environment [2]. From graphene to graphane, the electronic state changes from a semimetal to an insulator with a direct band gap of 3.5 eV. The hydrogenation of graphene is reversible [2], which provides the flexibility to manipulate the coverage of hydrogen. It is known that both graphene and graphane are nonmagnetic (NM). However, semihydrogenated graphene (graphone), with the hydrogen atoms on one side of graphane removed, was theoretically predicted to be a ferromagnetic (FM) semiconductor with a small indirect gap of 0.46 eV [3]. However, it was later revealed that the trigonal adsorption of hydrogen atoms in graphone is not stable; it evolves into rectangular adsorption geometry and turns into an antiferromagnetic (AFM) semiconductor with an indirect band gap of about 2.45 eV [4]. In addition, there are several works studying the electronic properties of graphene with various hydrogen distributions and concentrations [5–16]; it has been found that the electronic properties can be altered dramatically, e.g., opening a band gap, tuning the magnitude of the band gap of hydrogenated graphene by the hydrogen coverage, etc. Experimentally, room-temperature ferromagnetism was realized in hydrogenated epitaxial graphene [17,18]. Exploring other kinds of hydrogenated graphene with novel properties is the main purpose of the present work.

Searching for superconductivity in graphene is another long-time pursuit. Pure graphene is not a superconductor due to the vanishing density of states (DOS) at the Dirac point. Doping graphene can bring extra electrons/holes into the system, which may give rise to superconductivity. Actually, it was theoretically predicted [19] and, recently, experimentally confirmed [20] that Li-decorated graphene can dope the system with more electrons, enhance the electron-phonon coupling, and thus generate superconductivity. It was also theoretically studied that charge doping and tensile strain also induce conventional superconductivity in graphene [21]. Although graphane is an insulator with a large band gap, hole doping may turn it into a high-temperature electron-phonon superconductor [22]. In terms of the possible pairing symmetry of the superconducting (SC) graphene, singlet pairing, i.e., extended $s$ wave [23] or chiral $d$ wave in doped graphene (for a review see [24]), was theoretically suggested. There are also theoretical works on how to distinguish these two types of pairing symmetries [25,26]. In addition, there are also theories on possible $f$-wave triplet pairing at certain interaction strengths in the NM phase of doped graphene [27–29]. The possible existence of $p + ip$-wave triplet-pairing superconductivity in the FM graphene system is an emerging issue and so far has not been addressed.

Based on the above concerns and first-principles calculation, we show that two new hydrogenated graphene systems, $C_6H_1$ and $C_6H_5$, are, respectively, a FM semimetal and a FM semiconductor with a narrow gap of 0.7 eV separating the spin-up and the spin-down bands. We suggest that ferromagnetism and triplet-pairing superconductivity may coexist in doped $C_6H_1$ and $C_6H_5$. It is known that the coexistence of ferromagnetism and triplet-pairing superconductivity can be realized in $UGe_2$ [30,31], $ZrZn_2$ [32], URhGe [33], and UCoGe [34]. Therefore, $C_6H_1$ and $C_6H_5$ might provide another two fascinating platforms for studying the novel properties of the coexistence of ferromagnetism and triplet-pairing superconductivity.

*Lattice structure and stability.* The initial lattice structures of $C_6H_1$ and $C_6H_5$ are based on the graphene lattice. We adopt a periodic structure with six carbon atoms as a unit cell, and the basis vectors are along the armchair directions of carbon atoms, as can be seen in Fig. 1(a). Graphane will be generated if all six carbon atoms in the unit cell are bonded with hydrogen

*luhongyan2006@gmail.com

 

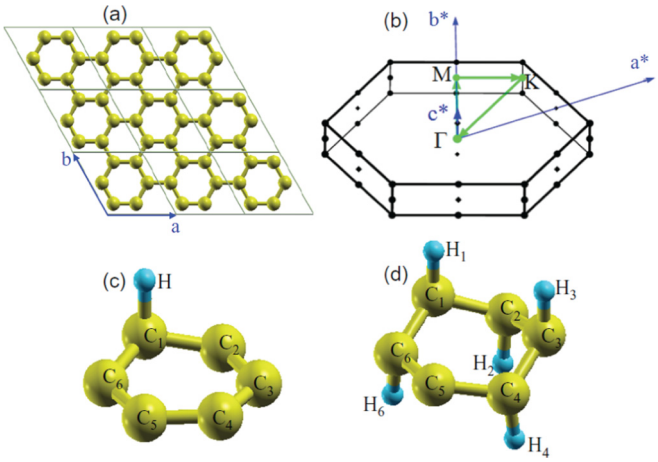


FIG. 1. (a) Periodic structure with six carbon atoms in a unit cell. $C_6H_1$ and $C_6H_5$ can be obtained by hydrogenating one or five carbon atoms in a unit cell. (b) The Brillouin zone and high-symmetry points for $C_6H_1$ and $C_6H_5$. (c) and (d) Optimized structure of $C_6H_1$ and $C_6H_5$ unit cells, in which the atoms are labeled to better describe their contributions.

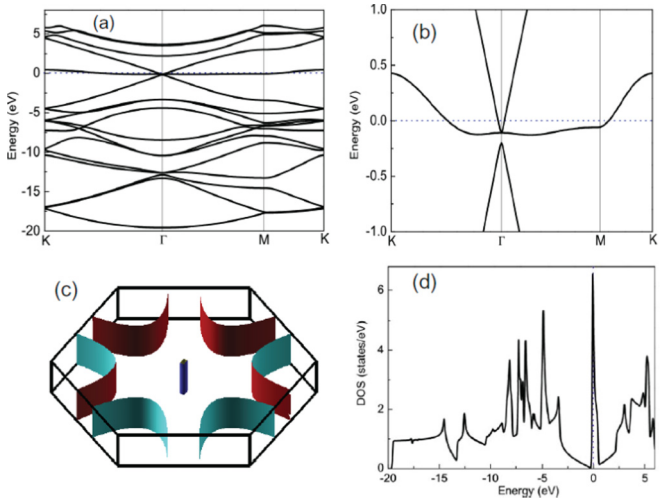


FIG. 2. Electronic structure of $C_6H_1$ in the non-spin-polarized case. (a) Electronic band structure along high-symmetry lines. The Fermi energy is set to be zero. (b) Electronic band structure around the Fermi energy. (c) FS sheets in the first BZ. (d) The total DOS.

atoms alternatively on both sides of the carbon plane and will further change to graphone if the hydrogen atoms on one side of the carbon plane are removed. In our case, $C_6H_1$ and $C_6H_5$ are obtained by hydrogenating one or five carbon atoms in a unit cell. The initial C-C bond length is set as 1.42 Å as in graphene, and the C-H bond length is set as 1.11 Å as in graphane [1]. A vacuum space of 20 Å normal to the graphene layer is used to avoid interactions between adjacent layers. The optimized unit-cell structures of $C_6H_1$ and $C_6H_5$ are shown in Figs. 1(c) and 1(d), respectively. The corresponding Brillouin zone (BZ) and high-symmetry points can be seen in Fig. 1(b). The calculation details and the bond lengths after relaxation are described in the Supplemental Material [35].

To prove the stability of $C_6H_1$ and $C_6H_5$, we calculate their formation energies. Using graphene and the hydrogen atom as a reference, as would be typical in the experimental setup [2,5–8], the formation energies for $C_6H_1$ and $C_6H_5$ are $-0.54$ and $-10.26$ eV per unit cell. The negative formation energies suggest that they are thermodynamically stable. The phonon spectra for the two systems are also calculated, and there are no imaginary frequencies, indicating that they are also dynamically stable [35].

*Electronic structure of* $C_6H_1$. In order to check the reliability of our methods, we calculate the fully and semihydrogenated cases in the 6-C unit cell. The obtained results are consistent with those reported for graphane [1] and graphone [3]. Then we present and discuss the numerical results for $C_6H_1$. We first show the results for a non-spin-polarized calculation. Figure 2(a) shows the band structure of $C_6H_1$ along high-symmetry lines $K$-Γ-$M$-$K$. Compared with the band structure of graphane, which is an insulator with a large gap [1], $C_6H_1$ is a semimetal. The most fascinating feature is that there exists a Dirac-cone-like structure with a gap of 0.23 eV at the Γ point, as shown in Fig. 2(b) with a small energy window near the Fermi level, and there is an almost flat band touching the bottom of the Dirac-cone band and crossing the Fermi energy away from the Γ point. For the corresponding Fermi surface (FS), Fig. 2(c) shows that there is no dispersion along the $k_z$ direction, confirming the two-dimensional characteristic of the electronic structure. It contains six large hole patches around the $K$ point and one small rectangular electron pocket around Γ point. The almost flat band will lead to a large DOS around the Fermi energy, as can be seen in Fig. 2(d). The DOS at the Fermi energy is located at a sharp Van Hove singularity peak, which indicates Stoner instability and may lead to a more stable spin-polarized state. Thus, we allow spin polarization in our calculations for $C_6H_1$. The calculated total and absolute magnetizations are nearly the same, with a value of $1\mu_B$/cell, suggesting that $C_6H_1$ is in FM state. By comparison, we find the total energy of the FM state is 0.093 eV/cell lower than that of the NM state, indicating the FM phase is the ground state of $C_6H_1$.

The electronic structure of $C_6H_1$ in the FM state is shown in Fig. 3. From Fig. 3(a), the spin polarization of the electronic states can be clearly seen; that is, the original bands in the NM state near the Fermi level now split into spin-up and spin-down channels. The spin-up channel moves downwards, whereas the spin-down channel moves upwards. To see it more clearly, we plot the band structure near the Fermi level in Fig. 3(b), which shows only two bands with up spin crossing the Fermi energy. This generates one electron pocket at the Γ point and six small hole patches at the $K$ points. The corresponding FS is plotted in Fig. 3(c). The above result confirms that $C_6H_1$ is a compensated semimetal; namely, the electron number and the hole number are identical. From the total DOS in Fig. 3(d), we can see the relevant charge carriers near the Fermi level in the spin-polarized $C_6H_1$ have up spins. Away from the Fermi level with $|E| > 1$ eV, the bands or the electron states have very little spin polarization. Also, to find which atoms contribute the most to the spin polarization, we plot the spin-polarized and orbital-projected DOSs for all the atoms, which are presented in the Supplemental Material [35]. It is found that the spin polarization comes mainly from the $2p_z$ orbitals of the $C_{2,4,6}$

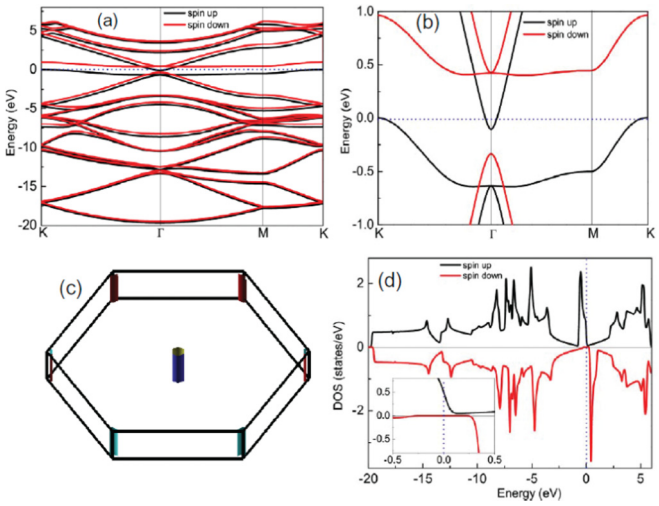


FIG. 3. Similar plot for $C_6H_1$ as in Fig. 2, but for spin-polarized calculations. The inset in (d) shows the DOS around the Fermi energy.

atoms, as seen in Fig. 1(c), i.e., the nearest neighbors of the hydrogenated carbon atoms.

*Electronic structure of* $C_6H_5$. The results are shown in Fig. 4. It is known that there is a large gap of 3.5 eV around the chemical potential for graphane. While for $C_6H_5$, it is equivalent to taking one hydrogen atom away from graphane (in the 6-C, 6-H unit cell), as shown in Fig. 1(d). The most obvious change in the band structure is that there is a narrow band crossing the Fermi level in the gap, as can be seen in Fig. 4(a). This almost flat band leads to a large DOS near the Fermi level [Fig. 4(b)], indicating that the NM state may be unstable against the formation of the spin-polarized state, similar to the case for $C_6H_1$. Therefore, we also do a spin-polarized calculation to determine the ground state. The calculated total and absolute magnetizations are also nearly the same, with a value of $1\mu_B$/cell, which also suggests $C_6H_5$ is in FM state. We further check that the total energy of the FM state is 0.233 eV/cell lower than that of the NM state, indicating that the FM state is the ground state of $C_6H_5$.

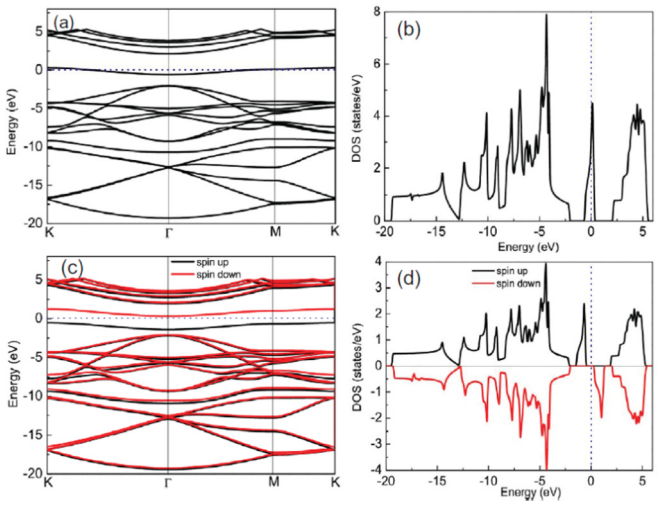


FIG. 4. The band structure and total DOS for $C_6H_5$. (a) and (b) Non-spin-polarized calculations and (c) and (d) spin-polarized calculations.

In the FM state of $C_6H_5$, Fig. 4(c) shows that the largest splitting of spin-up and spin-down bands occurs near the chemical potential. While the spin-up band moves below the chemical potential, the spin-down band increases above the chemical potential. There exists a small indirect gap of 0.7 eV separating the spin-up and the spin-down bands between the Γ point and the $K$ points. This can also be clearly seen from the DOS in Fig. 4(d). These results suggest that $C_6H_5$ is a FM semiconductor with a narrow band gap. But away from the chemical potential with $|E| > 1.5$ eV, the bands or the electron states have almost no spin polarization. Furthermore, to understand the origin of magnetism in $C_6H_5$, we plot the spin-polarized and orbital-projected electronic DOSs for each atom, which are also shown in the Supplemental Material [35]. The results show that the $2p_z$ orbital of the $C_5$ atom, i.e., the unhydrogenated carbon atom, contributes the most to the DOS around the chemical potential and the spin polarization.

*Possible* $p + ip$ *superconductivity in* $C_6H_1$ *and* $C_6H_5$. For $C_6H_1$, the electronic structure reveals that it is a FM semimetal, as shown in Figs. 3(a) and 3(b), with the chemical potential being set to zero. If we dope the sample with more electrons, for instance, by moving the chemical potential up to 0.25 eV, the hole pockets at the $K$ points disappear, and the electron pocket at the Γ point becomes enlarged. The corresponding FS is a cylinder around Γ, which is shown in Fig. 5(a). Similarly, if the system is doped with more holes by moving the chemical potential down to −0.25 eV, the electron pocket at the Γ point disappears, and the hole pockets at the $K$ points get enlarged. The FS for this case is presented in Fig. 5(b). The six patches at the $K$ points are equivalent to two quasicylindrical pockets around $K_1$ and $K_2$. In both the electron- and hole-doped cases, we have only spin-up charge carriers. If there exists any superconductivity in these systems, the pairing must be triplet. The pairing mechanism is usually dominated by the $p$-wave component of the pairing interactions, which may originate from the electron-phonon and the electron-magnon couplings. We start from a most natural $p$-wave pairing interaction,

$$H_p = \sum_{\mathbf{k},\mathbf{k}'} V_p(\mathbf{k},\mathbf{k}') c^\dagger_{\mathbf{k}\uparrow} c^\dagger_{-\mathbf{k}\uparrow} c_{-\mathbf{k}'\uparrow} c_{\mathbf{k}'\uparrow}, \tag{1}$$

in which the pairing potential $V_p(\mathbf{k},\mathbf{k}')$ respects the full $C_{3v}$ symmetry of this material. Explicitly,

$$V_p(\mathbf{k},\mathbf{k}') = \frac{2}{9\Omega} V_p^0 [\phi_1(\mathbf{k})\phi_1^*(\mathbf{k}') + \phi_2(\mathbf{k})\phi_2^*(\mathbf{k}') + \phi_3(\mathbf{k})\phi_3^*(\mathbf{k}')], \tag{2}$$

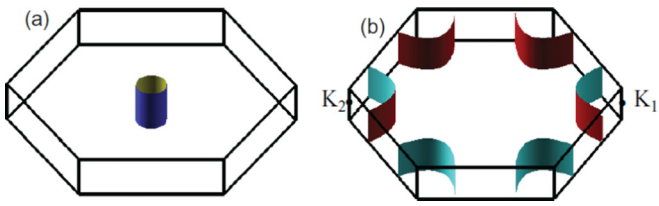


FIG. 5. FSs for electron- and hole-doped $C_6H_1$. The Fermi level moves (a) 0.25 eV upwards and (b) 0.25 eV downwards relative to the undoped case.

where $\Omega$ is the total area of the sample and $\phi_i(\mathbf{k})$ $(i = 1,2,3)$ are linear combinations of the basis of the twofold-degenerate $E$ representation of the $C_{3v}$ point group [36]. We have studied the leading pairing instabilities for both electron-doped and hole-doped materials.

For the electron-doped case, the pairing interaction is approximately expanded into the polynomial form as $V_p(\mathbf{k},\mathbf{k}') \sim k_x k_x' + k_y k_y'$. Define the mean-field order parameter as

$$\Delta(\mathbf{k}) = -\sum_{\mathbf{k}'} V_p(\mathbf{k},\mathbf{k}') \frac{\Delta(\mathbf{k}')}{E_{\mathbf{k}'}} \tanh \frac{\beta E_{\mathbf{k}'}}{2} = \Delta_\alpha \eta_\alpha(\mathbf{k}), \quad (3)$$

where $\alpha$ labels different pairing channels and $\Delta_\alpha$ is the constant pairing amplitude. Among three pairing channels characterized by symmetry factors $\eta_1(\mathbf{k}) = k_x$, $\eta_2(\mathbf{k}) = k_x + k_y$, and $\eta_3(\mathbf{k}) = k_x + ik_y$, the chiral third one is found to have the lowest ground-state energy and is thus the leading pairing instability (see the Supplementary Material for details [35]).

For the hole-doped case, the Fermi surface consists of two pockets around $K_1$ and $K_2$. It is necessary to make a comparison between interpocket BCS paring and intrapocket Fulde-Ferrell-Larkin-Ovchinnikov (FFLO) pairing [37,38]. It turns out that the leading BCS and leading FFLO pairings, which are both of the chiral $p + ip$ form, are degenerate if the two Fermi pockets are completely circular. However, in the actual system where the two Fermi pockets have only threefold symmetry, the phase space for the FFLO pairing is suppressed compared to that for the BCS pairing. Thus, the BCS $p + ip$ pairing is the leading pairing instability [35].

For $C_6H_5$, it is a FM semiconductor, as shown in Figs. 4(c) and 4(d). If we slightly dope it with more electrons or holes, for instance, by moving the chemical potential 0.5 eV upwards/downwards, we can obtain FSs similar to those of electron-/hole-doped $C_6H_1$, as shown in Figs. 5(a) and 5(b). For the electron-doped case, we have only spin-down charge carriers, and for the hole-doped case, we have only spin-up carriers. Therefore, if SC exists, it also has to show triplet-pairing symmetry. Since the $C_6H_5$ lattice also shows $C_{3v}$ symmetry and the FSs for doped $C_6H_5$ are similar to the doped $C_6H_1$ cases, we expect the pairing symmetries of the doped $C_6H_5$ are identical to those of doped $C_6H_1$.

*Discussion and conclusion.* The above interesting theoretical result, i.e., the coexistence of ferromagnetism and superconductivity with possible $p + ip$ pairing symmetry, is expected to stimulate further experimental synthesis of these two materials. Experimentally, many kinds of hydrogenated graphene systems have been reported. For example, graphane can be fabricated by exposing graphene in a hydrogen plasma environment [2]. More complicated systems are obtained by inducing patterned hydrogen chemisorption onto the moiré superlattice positions of graphene grown on an Ir (111) substrate [5] or on the basal plane of graphene on a SiC substrate [7]. Moreover, Lee *et al.* found that the electron beam from a scanning electron microscope can selectively remove hydrogen atoms [39]. Most importantly, stable two-dimensional $C_4H$ was experimentally synthesized [8]. There are many other investigations of various kinds of partially hydrogenated graphene systems (for a review, see Ref. [40]). Therefore, based on these experimental developments, we hope the proposed $C_6H_1$ and $C_6H_5$ may also be synthesized experimentally in the future.

If the disorder of H atoms exists in the two systems, it would definitely influence their properties. However, based on the above experiments, the disorder can be maximally controlled. In view of the previous theoretical works on other similar systems, such as graphane [1], graphone [3], $C_4H$ [8], single-side-hydrogenated graphene [16], doped graphane [22], etc., all of which were studied with ideal periodic structures, we thus consider only the periodic cases.

Doping could be achieved experimentally by gating, including using an electrolyte gate, or by charge transfer, as done in graphene [41–43]. For graphane, hole doping can be obtained by partially substituting carbon atoms with boron atoms [22]. It showed that the band structure and the DOS of graphane near the chemical potential inside and outside the band gap are practically unchanged even up to a 12.5% boron doping. This justifies the use of a rigid-band approximation to simulate substitutional doping in graphane. The above work demonstrated that small substitutional dopings shift only the chemical potential and do not change the band structure near the chemical potential. Our current doping is less than 1.6% hole or electron doping, which will also not change the band structure. Of course, even if the dopants are randomly distributed, they should have negligible effect on the band structure at such a small concentration.

Finally, we would like to make a comparison between the triplet-pairing superconductivity in $C_6H_1/C_6H_5$ systems and those in heavy-metal ($UGe_2$ [30,31], URhGe [33], and UCoGe [34]) or transition-metal-based metallic compounds. All of them show the coexistence of triplet-pairing superconductivity and itinerant electron ferromagnetism but originate from different electron orbitals. For uranium-based systems, ferromagnetism and the superconductivity are determined by the U $5f$ orbitals with possible strong spin-orbital couplings. However, for the transition-metal-based system $ZrZn_2$ [32], Zr $4d$ orbital electrons play the most important role. Therefore, the predicted $C_6H_1/C_6H_5$ may provide new platforms to study the coexistence of ferromagnetism and triplet-pairing superconductivity within $p$ electron orbitals.

In conclusion, we predicted two new types of hydrogenated graphene, $C_6H_1$ and $C_6H_5$, and found they are a FM semimetal and a FM semiconductor with a narrow gap, respectively. For doped $C_6H_1$ and $C_6H_5$, there may exist superconductivity with chiral $p + ip$ pairing symmetry, which is known to support chiral edge states and vortex zero modes, both known as Majorana fermions [44,45]. Thus, the predicted superconducting phases for $C_6H_1$ and $C_6H_5$ may provide new platforms for studying the novel physics in topological quantum computations [46].

*Acknowledgments.* We are thankful for helpful discussions with J.-X. Zhu, V. G. Hadjiev, S.-Y. Lin, and R. Thomale. This work is supported by the Texas Center for Superconductivity at the University of Houston and the Robert A. Welch Foundation (Grant No. E-1146), the National Natural Science Foundation of China (Grants No. 11574108, No. 11104099, and No. 11204035), the Natural Science Foundation of Anhui Province (Grant No. 1408085QA12), and the Natural Science Research

Project of Higher Education Institutions of Anhui Province (Grant No. KJ2015A120). The numerical calculations were performed at the Center of Advanced Computing and Data Systems at the University of Houston.

[1] J. O. Sofo, A. S. Chaudhari, and G. D. Barber, Phys. Rev. B **75**, 153401 (2007).
[2] D. C. Elias, R. R. Nair, T. M. G. Mohiuddin, S. V. Morozov, P. Blake, M. P. Halsall, A. C. Ferrari, D. W. Boukhvalov, M. I. Katsnelson, A. K. Geim, and K. S. Novoselov, Science **323**, 610 (2009).
[3] J. Zhou, Q. Wang, Q. Sun, X. S. Chen, Y. Kawazoe, and P. Jena, Nano Lett. **9**, 3867 (2009).
[4] L. Feng and W. X. Zhang, AIP Adv. **2**, 042138 (2012).
[5] R. Balog, B. Jørgensen, L. Nilsson, M. Andersen, E. Rienks, M. Bianchi, M. Fanetti, E. Lægsgaard, A. Baraldi, S. Lizzit, Z. Sljivancanin, F. Besenbacher, B. Hammer, T. G. Pedersen, P. Hofmann, and L. Hornekær, Nat. Mater. **9**, 315 (2010).
[6] M. Jaiswal, C. H. Y. X. Lim, Q. Bao, C. T. Toh, K. P. Loh, and B. Özyilmaz, ACS Nano **5**, 888 (2011).
[7] R. Balog, B. Jørgensen, J. Wells, E. Lægsgaard, P. Hofmann, F. Besenbacher, and L. Hornekær, J. Am. Chem. Soc. **131**, 8744 (2009).
[8] D. Haberer, C. E. Giusca, Y. Wang, H. Sachdev, A. V. Fedorov, M. Farjam, S. A. Jafari, D. V. Vyalikh, D. Usachov, X. Liu, U. Treske, M. Grobosch, O. Vilkov, V. K. Adamchuk, S. Irle, S. R. P. Silva, M. Knupfer, B. Büchner, and A. Grüneis, Adv. Mater. **23**, 4497 (2011).
[9] P. Chandrachud, B. S. Pujari, S. Haldar, B. Sanyal, and D. G. Kanhere, J. Phys. Condens. Matter **22**, 465502 (2010).
[10] M. Yang, A. Nurbawono, C. Zhang, Y. P. Feng, and Ariando, Appl. Phys. Lett. **96**, 193115 (2010).
[11] H. Gao, L. Wang, J. Zhao, F. Ding, and J. Lu, J. Phys. Chem. C **115**, 3236 (2011).
[12] H.-C. Huang, S.-Y. Lin, C.-L. Wu, and M.-F. Lin, Carbon **103**, 84 (2016).
[13] P. O. Lehtinen, A. S. Foster, Y. Ma, A. V. Krasheninnikov, and R. M. Nieminen, Phys. Rev. Lett. **93**, 187202 (2004).
[14] S. Casolo, O. M. Løvvik, R. Martinazzo, and G. F. Tantardini, J. Chem. Phys. **130**, 054704 (2009).
[15] E. J. Duplock, M. Scheffler, and P. J. D. Lindan, Phys. Rev. Lett. **92**, 225502 (2004).
[16] B. S. Pujari, S. Gusarov, M. Brett, and A. Kovalenko, Phys. Rev. B **84**, 041402(R) (2011).
[17] L. Xie, X. Wang, J. Lu, Z. Ni, Z. Luo, H. Mao, R. Wang, Y. Wang, H. Huang, D. Qi, R. Liu, T. Yu, Z. Shen, T. Wu, H. Peng, B. Özyilmaz, K. Loh, A. T. S. Wee, Ariando, and W. Chen, Appl. Phys. Lett. **98**, 193113 (2011).
[18] A. J. M. Giesbers, K. Uhlířová, M. Konečný, E. C. Peters, M. Burghard, J. Aarts, and C. F. J. Flipse, Phys. Rev. Lett. **111**, 166101 (2013).
[19] G. Profeta, M. Calandra, and F. Mauri, Nat. Phys. **8**, 131 (2012).
[20] B. M. Ludbrook, G. Levy, P. Nigge, M. Zonno, M. Schneider, D. J. Dvorak, C. N. Veenstra, S. Zhdanovich, D. Wong, P. Dosanjh, C. Straßer, A. Stöhr, S. Forti, C. R. Ast, U. Starke, and A. Damascelli, Proc. Natl. Acad. Sci. USA **112**, 11795 (2015).
[21] C. Si, Z. Liu, W. Duan, and F. Liu, Phys. Rev. Lett. **111**, 196802 (2013).
[22] G. Savini, A. C. Ferrari, and F. Giustino, Phys. Rev. Lett. **105**, 037002 (2010).
[23] B. Uchoa and A. H. Castro Neto, Phys. Rev. Lett. **98**, 146801 (2007).
[24] A. M. Black-Schaffer and C. Honerkamp, J. Phys. Condens. Matter **26**, 423201 (2014).
[25] H.-Y. Lu, S. Chen, Y. Xu, L.-Q. Zhang, D. Wang, and W.-S. Wang, Phys. Rev. B **88**, 085416 (2013).
[26] Y. Jiang, D.-X. Yao, E. W. Carlson, H.-D. Chen, and J. P. Hu, Phys. Rev. B **77**, 235420 (2008).
[27] C. Honerkamp, Phys. Rev. Lett. **100**, 146404 (2008).
[28] M. L. Kiesel, C. Platt, W. Hanke, D. A. Abanin, and R. Thomale, Phys. Rev. B **86**, 020507(R) (2012).
[29] R. Nandkishore, R. Thomale, and A. V. Chubukov, Phys. Rev. B **89**, 144501 (2014).
[30] S. S. Saxena, P. Agarwal, K. Ahilan, F. M. Grosche, R. K. W. Haselwimmer, M. J. Steiner, E. Pugh, I. R. Walker, S. R. Julian, P. Monthoux, G. G. Lonzarich, A. Huxley, I. Sheikin, D. Braithwaite, and J. Flouquet, Nature (London) **406**, 587 (2000).
[31] K. Machida and T. Ohmi, Phys. Rev. Lett. **86**, 850 (2001).
[32] C. Pfleiderer, M. Uhlarz, S. M. Hayden, R. Vollmer, H. v. Löhneysen, N. R. Bernhoeft, and G. G. Lonzarich, Nature (London) **412**, 58 (2001).
[33] D. Aoki, A. Huxley, E. Ressouche, D. Braithwaite, J. Flouquet, J.-P. Brison, E. Lhotel, and C. Paulsen, Nature (London) **413**, 613 (2001).
[34] N. T. Huy, A. Gasparini, D. E. de Nijs, Y. Huang, J. C. P. Klaasse, T. Gortenmulder, A. de Visser, A. Hamann, T. Görlach, and H. v. Löhneysen, Phys. Rev. Lett. **99**, 067006 (2007).
[35] See Supplemental Material http://link.aps.org/supplemental/10.1103/PhysRevB.93.241410 for the details of computational methods, bond lengths, phonon spectra, spin-polarized and orbital-projected electronic DOSs, and the superconductivity instabilities.
[36] M. S. Dresselhaus, G. Dresselhaus, and A. Jorio, *Group Theory: Application to the Physics of Condensed Matter* (Springer, Berlin, 2008).
[37] P. Fulde and R. A. Ferrell, Phys. Rev. **135**, A550 (1964).
[38] A. I. Larkin and Y. N. Ovchinnikov, Zh. Eksp. Teor. Fiz. **47**, 1136 (1964) [Sov. Phys. JETP **20**, 762 (1965)].
[39] W.-K. Lee, K. E. Whitener, Jr., J. T. Robinson, and P. E. Sheehan, Adv. Mater. **27**, 1774 (2015).
[40] H. Sahin, O. Leenaerts, S. K. Singh, and F. M. Peeters, WIREs Comput. Mol. Sci. **5**, 255 (2015).
[41] A. Das, S. Pisana, B. Chakraborty, S. Piscanec, S. K. Saha, U. V. Waghmare, K. S. Novoselov, H. R. Krishnamurhthy, A. K. Geim, A. C. Ferrari, and A. K. Sood, Nat. Nanotechnol. **3**, 210 (2008).
[42] I. Gierz, C. Riedl, U. Starke, C. R. Ast, and K. Kern, Nano Lett. **8**, 4603 (2008).
[43] N. Jung, N. Kim, S. Jockusch, N. J. Turro, P. Kim, and L. Brus, Nano Lett. **9**, 4133 (2009).
[44] N. Read and D. Green, Phys. Rev. B **61**, 10267 (2000).
[45] D. A. Ivanov, Phys. Rev. Lett. **86**, 268 (2001).
[46] C. Nayak, S. H. Simon, A. Stern, M. Freedman, and S. D. Sarma, Rev. Mod. Phys. **80**, 1083 (2008).